Supplemental Information

Structural Basis of Alcohol Inhibition of the Pentameric Ligand-gated Ion Channel ELIC

Qiang Chen, Marta M. Wells, Tommy S. Tillman, Monica N. Kinde, Aina Cohen, Yan Xu, Pei Tang

EXPERIMENTAL DETAILS, related to EXPERIMENTAL PROCEDURES

Protein expression and purification

ELIC was expressed using a plasmid generously provided by Professor Raimund Dutzler's lab of the University of Zürich (Hilf and Dutzler, 2008) and purified as reported previously (Chen et al., 2015; Kinde et al., 2015; Pan et al., 2012b). Briefly, ELIC was transformed to Rosetta (DE3) pLysS (Novagen) cells for expression at 15°C for 24 hours. The expression was induced with 0.2 mM isopropyl β-D-1-thiogalactopyranoside in M9 media. Harvested cells were re-suspended in a buffer (50 mM sodium phosphate at pH 8, 150 mM NaCl, and protease inhibitors) and lysed using a M-110Y microfluidizer processor (Microfluidics). Cell membrane was pelleted by ultracentrifugation. The fusion protein was extracted with 3.5% (w/v) *n*-undecyl-β-D-maltoside (Anatrace) and purified with a 5-ml HisTrap HP column (GE Healthcare). Maltose binding protein was cleaved overnight using protease HRV3C (GE Healthcare) and separated from ELIC using HisTrap HP columns. The pentameric ELIC was collected in a buffer containing 10 mM sodium phosphate at pH8, 150 mM NaCl, 0.025% (w/v) n-dodecyl-β-D-maltoside (Anatrace) by size exclusion chromatography using a Superdex 200 10/300GL column (GE Healthcare). The purified pentameric ELIC was concentrated to 5 ~ 6 mg/ml for crystallization.

Crystallography and data analysis

Crystallization was set up at 4°C using the sitting-drop plate (Hampton Research). All chemicals used for crystallization were purchased from Sigma-Aldrich (St. Louis, MO) unless stated otherwise. BrEtOH (100 mM) was mixed with ELIC for at least 30 minutes in the presence of 0.01~0.02 mg/ml *E. coli* polar lipids (Avanti Polar Lipids). The agonist propylamine (5 mM) was also added to ELIC to produce a desensitized condition in some of the samples. The reservoir solution (10-12% PEG 4000, 200 mM ammonium sulfate, 100 mM MES buffer at pH 6.1) was then added to the protein mixture in 1:1 ratio during crystallization setup. Crystals were formed after one to two weeks and harvested in liquid nitrogen after cryo-protection with up to 20% glycerol.

The X-ray diffraction data were collected on beamline 12-2 at the Stanford Synchrotron Radiation Lightsource (SSRL) with a PILATUS 6M detector. The anomalous scattering was acquired near the Br K-edge peak. The data were indexed, integrated, and scaled with the XDS program (Kabsch, 2010).

A previously published ELIC structure (PDB code: 3RQU) was used as a starting template for the structure determination of BrEtOH-bound ELIC in the presence and absence of the agonist propylamine. Two regions in 3RQU, including residues 136-156 and residues 285-295, were rebuilt to improve the fitting of electron density. The resulting model was refined iteratively using Phenix (Adams et al., 2010) and Coot (Emsley et al., 2010). The binding sites of BrEtOH were determined based on the bromine-specific (0.9195 Å) anomalous difference map. The whole BrEtOH molecule was built to fit the Fo-Fc difference density using the program Coot (Emsley et al., 2010). The initial BrEtOH structure was obtained from a published GLIC complex structure (PDB code: 4HFC) (Sauguet et al., 2013). The refined BrEtOH in ELIC was in an energy favored gauche conformation (Thomassen et al., 1993). The geometry and stereochemistry of each model were validated by MolProbility (Davis et al., 2004). Automatic solvent detection, updating, and refinement were conducted for placing water molecules and followed by manual inspection and adjustment. Torsional non-crystallographic symmetry (NCS) restraints were applied to all subunits of two pentamers in the asymmetric unit. The final structures were analyzed using Phenix (Adams et al., 2010) and all molecular graphics were prepared using PyMol (DeLano, 2002).

Electrophysiology

Two-electrode voltage clamping (TEVC) was used to measure the functional responses of *Xenopus laevis* oocytes expressing ELIC, its mutants, and the ELIC-$GABA_AR$ chimeras to n-alcohols. All the procedures involving *Xenopus laevis* oocytes were approved by the University of Pittsburgh Institutional Animal Care and Use Committee. DNA encoding ELIC was inserted downstream of a T7 promoter in the pCMV-mGFP Cterm S11 Neo Kan vector (Theranostech, NM). Site-directed mutagenesis was introduced using the QuickChange Lightning Kit (Agilent). ELIC-α1β3$GABA_AR$ was constructed using overlapping PCR by fusing the ECD ending at R199 of ELIC with the TMD of the α1$GABA_AR$ starting at K222 or the β3$GABA_AR$ starting at N217. The resulting constructs were

subcloned to the pCMV-mGFP Cterm S11 Neo Kan vector and confirmed by sequencing. cRNA preparation, protein expression in *Xenopus laevis* oocytes, and electrophysiology measurements followed the same protocols as reported previously (Kinde et al., 2015 Wells, 2015 #165; Pan et al., 2012a; Pan et al., 2012b; Tillman et al., 2013; Tillman et al., 2014). Oocytes were clamped to a holding potential of -40 or -60 mV. The recording solutions contained 130 mM NaCl, 0.1 mM $CaCl_2$, 10 mM HEPES, pH 7.0 as well as desired concentrations of alcohols and propylamine. Short chain alcohols up to n-hexanol were dissolved directly in the buffer. The long chain alcohols *n*-nonanol, *n*-decanol, and *n*-dodecanol were dissolved in DMSO first before diluted in the buffer with a final DMSO concentration less than 0.05%. Data were collected and processed using Clampex 10 (Molecular Devices). Non-linear regressions were performed using Prism 5.0 (Graphpad).

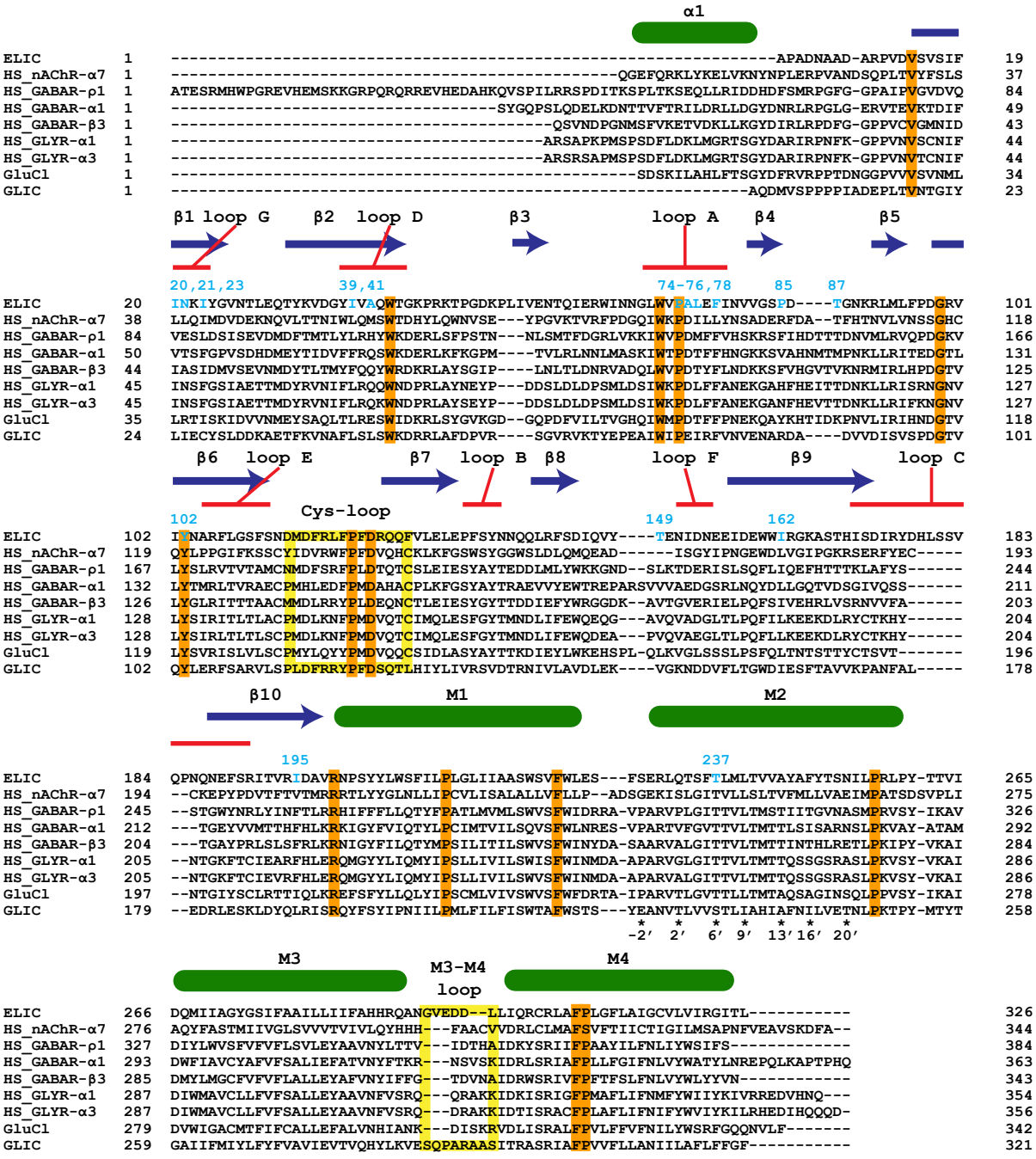

Figure S1, related to Figure 2, 3: Sequence alignment of ELIC, human α7nAChR, and human ρ1GABA$_A$R and other pLGICs. The residues involved in the Br-EtOH binding sites of ELIC are marked with their sequence numbers (cyan). The pore-lining residue T237(6′) is conserved among all channels except GLIC. All of the pore-lining residues are marked with ★ and conventional position numbers. The conserved residues are highlighted in orange color. Secondary structures of helices (green bars), beta sheets (blue arrows), and the loops (red lines) are also marked above the sequences. PROMASL3D (Pei et al., 2008) was used for the sequence alignment.

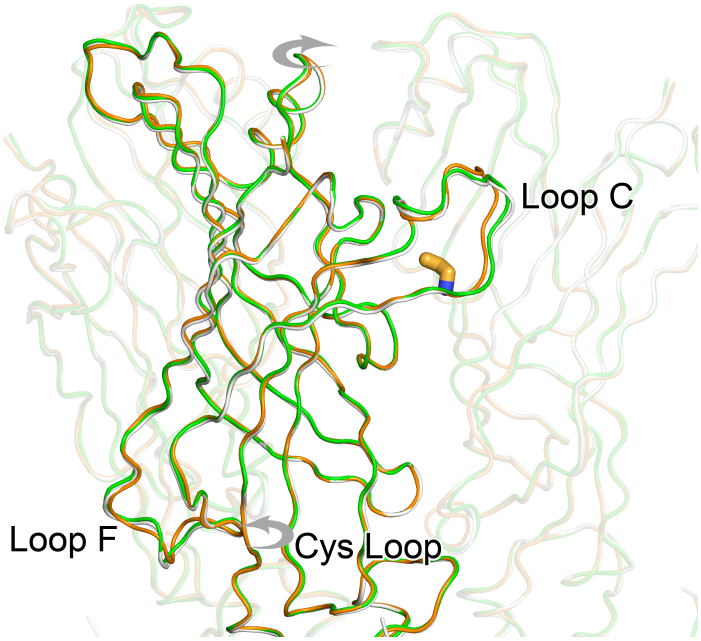

Figure S2, related to Figure 2, 3. Motion in the extracellular domain of ELIC upon binding of the agonist PPA. Superposition of the backbone structures: Apo ELIC (white, PDB code: 3RQU), ELIC bound BrEtOH in the absence of the agonist PPA (green, PDB code: 5SXV), and ELIC bound BrEtOH in the presence of PPA (orange, PDB code: 5SXU). The binding of PPA causes counterclockwise rotation or inward movement of Loop C. The maximum displacement is 1.5 Å as measured by Cα distances in the alligned structures. For clarity, only one of the ELIC subunits is highlighted.

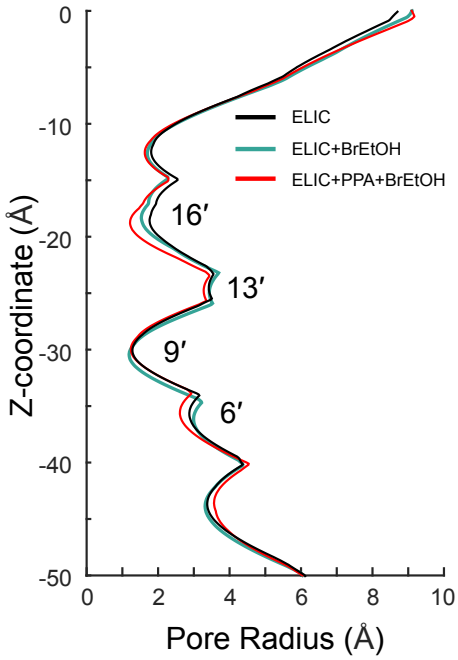

Figure S3, related to Figure 2, 3. Pore radius profiles of ELIC calculated from crystal structures obtained under three crystallization conditions: Apo ELIC (black, PDB code: 3RQU), ELIC bound BrEtOH in the absence of the agonist propylamine (PPA) (green, PDB code: 5SXV), and ELIC bound BrEtOH in the presence of PPA (red, PDB code: 5SXU). The pore profiles were calculated using the HOLE program (Smart et al., 1993). The BrEtOH binding introduced only ~0.5 Å or less changes in the pore radius.

Table S1, related to Figure 1

IC_{50} and Hill coefficients (n_H) of *n*-alcohols measured on ELIC and the comparisons with IC_{50} and EC_{50} measured on other pLGICs and tadpoles.

Alcohols	**ELIC**		**pLGICs**	**Anesthetic potencies for tadpoles**
	IC_{50} (mM)	**n_H**	**IC_{50} (mM)**	**EC_{50} (mM)**
EtOH	52.1 ± 1.5*	1.55 ± 0.06	ρ1GABA$_A$R, 83[1]; α7nAChR, 33[2]	190 ± 16[5]
BrEtOH	11.5 ± 0.4*	1.66 ± 0.09		
n-Propanol	2.45 ± 0.14	1.43 ± 0.12		
n-Butanol	1.45 ± 0.08	1.06 ± 0.06	ρ1GABA$_A$R, 6~7[1#]; α3β2nAChR, 39.7 ± 2.0[3]; GLIC, ~10[4] (Howard et al., 2011)	10.8 ± 0.77[5]
n-Hexanol	0.36 ± 0.02	1.09 ± 0.07	ρ1GABA$_A$R, ~2[1#]; α3β2nAChR, 1.12 ± 0.09[3]	0.570 ± 0.037[5] (Alifimoff et al., 1989)
n-Nonanol	0.15 ± 0.01	0.83 ± 0.05	ρ1GABA$_A$R, ~0.6[1#]**;** GLIC, 0.001[4]	0.037 ± 0.002[5]

IC_{50} and Hill coefficients are expressed as mean ± sem. Note that the standard errors (sem) reported by Prism (and virtually all other nonlinear regression programs) are based on some mathematical simplifications. They are called "asymptotic" or "approximate" standard errors. [#]IC_{50} is estimated from Fig.2 in the reference (Mihic and Harris, 1996). [1](Mihic and Harris, 1996), [2](Yu et al., 1996), [3](Zuo et al., 2002), [4](Howard et al., 2011), and [5](Alifimoff et al., 1989)

***** A slightly larger molecular size and higher hydrophobicity of BrEtOH (72.14 Å^3; miLogP 0.42) than EtOH (54.02 Å^3; miLogP 0.06) may have contributed to the decreased IC_{50} for BrEtOH over EtOH. miLogP is Molinspiration calculated logP. Octanol-water partition coefficient logP is used as a measure of molecular hydrophobicity (http://www.molinspiration.com/).

REFERENCES

Adams, P.D., Afonine, P.V., Bunkoczi, G., Chen, V.B., Davis, I.W., Echols, N., Headd, J.J., Hung, L.W., Kapral, G.J., Grosse-Kunstleve, R.W., *et al.* (2010). PHENIX: a comprehensive Python-based system for macromolecular structure solution. Acta Crystallogr D Biol Crystallogr *66*, 213-221.

Alifimoff, J.K., Firestone, L.L., and Miller, K.W. (1989). Anaesthetic potencies of primary alkanols: implications for the molecular dimensions of the anaesthetic site. Br J Pharmacol *96*, 9-16.

Chen, Q., Kinde, M.N., Arjunan, P., Wells, M.M., Cohen, A.E., Xu, Y., and Tang, P. (2015). Direct Pore Binding as a Mechanism for Isoflurane Inhibition of the Pentameric Ligand-gated Ion Channel ELIC. Sci Rep *5*, 13833.

Davis, I.W., Murray, L.W., Richardson, J.S., and Richardson, D.C. (2004). MOLPROBITY: structure validation and all-atom contact analysis for nucleic acids and their complexes. Nucleic Acids Res *32*, W615-619.

DeLano, W.L. (2002). The PyMOL Molecular Graphics System, Schrödinger, LLC. (Palo Alto, CA, Delano Scientific LLC).

Emsley, P., Lohkamp, B., Scott, W.G., and Cowtan, K. (2010). Features and development of Coot. Acta Crystallogr D Biol Crystallogr *66*, 486-501.

Hilf, R.J., and Dutzler, R. (2008). X-ray structure of a prokaryotic pentameric ligand-gated ion channel. Nature *452*, 375-379.

Howard, R.J., Murail, S., Ondricek, K.E., Corringer, P.J., Lindahl, E., Trudell, J.R., and Harris, R.A. (2011). Structural basis for alcohol modulation of a pentameric ligand-gated ion channel. Proc Natl Acad Sci U S A *108*, 12149-12154.

Kabsch, W. (2010). Xds. Acta Crystallogr D Biol Crystallogr *66*, 125-132.

Kinde, M.N., Chen, Q., Lawless, M.J., Mowrey, D.D., Xu, J., Saxena, S., Xu, Y., and Tang, P. (2015). Conformational Changes Underlying Desensitization of the Pentameric Ligand-Gated Ion Channel ELIC. Structure *23*, 995-1004.

Mihic, S.J., and Harris, R.A. (1996). Inhibition of rho1 receptor GABAergic currents by alcohols and volatile anesthetics. J Pharmacol Exp Ther *277*, 411-416.

Pan, J., Chen, Q., Willenbring, D., Mowrey, D., Kong, X.P., Cohen, A., Divito, C.B., Xu, Y., and Tang, P. (2012a). Structure of the pentameric ligand-gated ion channel GLIC bound with anesthetic ketamine. Structure *20*, 1463-1469.

Pan, J., Chen, Q., Willenbring, D., Yoshida, K., Tillman, T., Kashlan, O.B., Cohen, A., Kong, X.P., Xu, Y., and Tang, P. (2012b). Structure of the pentameric ligand-gated ion channel ELIC cocrystallized with its competitive antagonist acetylcholine. Nat Commun *3*, 714.

Pei, J., Tang, M., and Grishin, N.V. (2008). PROMALS3D web server for accurate multiple protein sequence and structure alignments. Nucleic Acids Res *36*, W30-34.

Sauguet, L., Howard, R.J., Malherbe, L., Lee, U.S., Corringer, P.J., Harris, R.A., and Delarue, M. (2013). Structural basis for potentiation by alcohols and anaesthetics in a ligand-gated ion channel. Nat Commun *4*, 1697.

Smart, O.S., Goodfellow, J.M., and Wallace, B.A. (1993). The pore dimensions of gramicidin A. Biophys J *65*, 2455-2460.

Thomassen, H., Samdal, S., and Hedberg, K. (1993). Conformational-Analysis .20. 2-Bromoethanol and 2-Iodoethanol - Structures, Compositions, and Anti-Gauche Energy and Entropy Differences from Electron-Diffraction and Structures and Vibrational Wave-Numbers from an Abinitio Calculation. J Phys Chem *97*, 4004-4010.

Tillman, T., Cheng, M.H., Chen, Q., Tang, P., and Xu, Y. (2013). Reversal of ion-charge selectivity renders the pentameric ligand-gated ion channel GLIC insensitive to anaesthetics. Biochem J *449*, 61-68.

Tillman, T.S., Seyoum, E., Mowrey, D.D., Xu, Y., and Tang, P. (2014). ELIC-alpha7 Nicotinic acetylcholine receptor (alpha7nAChR) chimeras reveal a prominent role of the extracellular-transmembrane domain interface in allosteric modulation. J Biol Chem *289*, 13851-13857.

Yu, D., Zhang, L., Eisele, J.L., Bertrand, D., Changeux, J.P., and Weight, F.F. (1996). Ethanol inhibition of nicotinic acetylcholine type alpha 7 receptors involves the amino-terminal domain of the receptor. Mol Pharmacol *50*, 1010-1016.

Zuo, Y., Kuryatov, A., Lindstrom, J.M., Yeh, J.Z., and Narahashi, T. (2002). Alcohol modulation of neuronal nicotinic acetylcholine receptors is alpha subunit dependent. Alcohol Clin Exp Res *26*, 779-784.